OPTICA

On-chip optical levitation with a metalens in vacuum

Kunhong Shen,[1] Yao Duan,[2] Peng Ju,[1] Zhujing Xu,[1] Xi Chen,[2] Lidan Zhang,[2] Jonghoon Ahn,[3] Xingjie Ni,[2,6] and Tongcang Li[1,3,4,5,7]

[1]Department of Physics and Astronomy, Purdue University, West Lafayette, Indiana 47907, USA
[2]Department of Electrical Engineering, The Pennsylvania State University, University Park, Pennsylvania 16802, USA
[3]School of Electrical and Computer Engineering, Purdue University, West Lafayette, Indiana 47907, USA
[4]Birck Nanotechnology Center, Purdue University, West Lafayette, Indiana 47907, USA
[5]Purdue Quantum Science and Engineering Institute, Purdue University, West Lafayette, Indiana 47907, USA
[6]e-mail: xingjie@psu.edu
[7]e-mail: tcli@purdue.edu

Received 22 July 2021; revised 4 September 2021; accepted 5 September 2021 (Doc. ID 438410); published 21 October 2021

Optical levitation of dielectric particles in vacuum is a powerful technique for precision measurements, testing fundamental physics, and quantum information science. Conventional optical tweezers require bulky optical components for trapping and detection. Here, we design and fabricate an ultrathin dielectric metalens with a high numerical aperture of 0.88 at 1064 nm in vacuum. It consists of 500-nm-thick silicon nano-antennas, which are compatible with an ultrahigh vacuum. We demonstrate optical levitation of nanoparticles in vacuum with a single metalens. The trapping frequency can be tuned by changing the laser power and polarization. We also transfer a levitated nanoparticle between two separated optical tweezers. Optical levitation with an ultrathin metalens in vacuum provides opportunities for a wide range of applications including on-chip sensing. Such metalenses will also be useful for trapping ultracold atoms and molecules.

https://doi.org/10.1364/OPTICA.438410

There has been remarkable progress in levitated optomechanics over the past decade [1], including ultrasensitive force (10^{-21}N) and torque (10^{-28}Nm) detection [2,3], acceleration sensing [4], mass measurement [5], ultrafast rotation [3,6,7], chemical nanoreactor [8], optical refrigeration [9], quantum ground-state cooling [10], and testing fundamental physics. Several schemes have been proposed for utilizing optical levitation systems in vacuum to study Casimir physics [11], quantum aspects of gravity [12], and search for dark matter and dark energy [13]. Typically, optical trapping of a nanoparticle in vacuum uses a bulky objective lens (OBJ) with a large numerical aperture (NA) to tightly focus a laser beam [3,6,7]. If the NA of the focusing lens is not high enough, a pair of lenses would be required to focus two counter-propagating laser beams for creating a stable three-dimensional (3D) trap without the help of gravity [2]. The system is usually bulky and inconvenient for practical applications of optically levitated particles, such as accelerometers. Minimizing the focusing lens and levitating a dielectric particle on chip are on demand for realizing compact levitated optomechanical systems with high performance and efficiency. Here, we report on-chip optical levitation of nanoparticles in vacuum with an ultrathin nanofabricated metalens.

An optical metasurface is a recent breakthrough in optics [14]. It uses nanostructures to achieve unprecedented control of light properties [15]. A metalens may be created by arranging phase-shifting elements on a surface that forms a phase profile of a lens [16,17]. Optical trapping in liquids-based metalenses were demonstrated recently [18–20]. Optical manipulation and trapping by a metalens show high flexibility for being integrated to a chip-based device and fluid cells. However, metalens optical traps have only been carried out in liquids so far [18–20], which limits the scope of applications. The largest full angular aperture of the metalenses used in these trapping experiments is 85°, corresponding to an NA of 0.9 in water [20]. Because the nonconservative scattering force increases faster than the gradient force when the contrast of the refractive index increases, single-beam optical trapping of a nanoparticle in vacuum requires a focusing lens with a larger angular aperture than that in a liquid [21]. In addition, the metalens should have high efficiency and low absorption to avoid laser heating in vacuum. To the best of our knowledge, there has been no report on optical levitation of particles with a metalens in air or vacuum.

In this Letter, we report the realization of on-chip optical levitation in vacuum with a high-NA metalens (Fig. 1). We design and fabricate planar metalenses with silicon nanopillars on a sapphire substrate. The full angular aperture of our metalens is 123°, corresponding to a measured NA of 0.88 in air. We levitate a nanoparticle by optical tweezers generated with a single metalens at a pressure of 2×10^{-4} Torr without feedback cooling. We then transfer a nanoparticle between two optical tweezers separated by about 1.5 μm.

We first design and fabricate a high-NA metalens for levitating a nanoparticle in vacuum [Fig. 1(a)]. Assuming the incident laser propagates along the z axis, a high-NA lens should have an aspheric phase shift of $\phi(x, y) = 2\pi/\lambda \cdot (f - \sqrt{x^2 + y^2 + f^2}) + \phi_0$, where λ is the wavelength, f is the focal length, and ϕ_0 is an overall

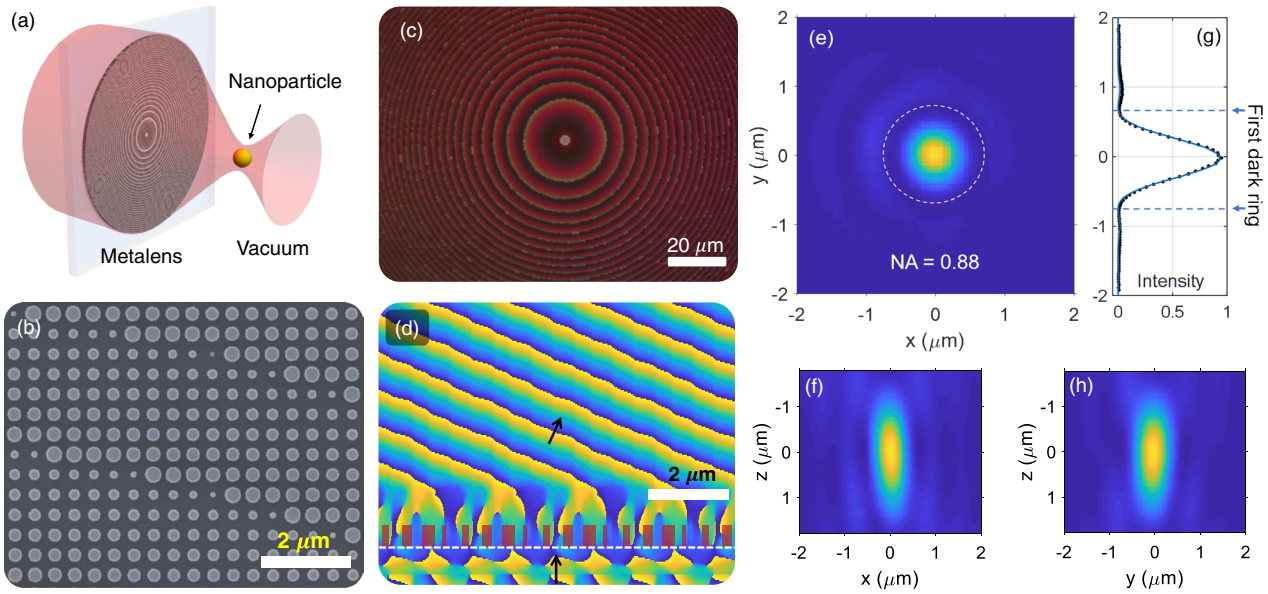

Fig. 1. (a) Schematic of an optically levitated nanoparticle with a metalens in vacuum. (b) A SEM image of the metalens antennas, which are silicon nanopillars with a height of 500 nm. (c) An optical image of a metalens. (d) One-dimensional phase simulation of a beam passing through the antennas. The antennas are shown as brown pillars, and the substrate surface of the metalens is denoted by the white dashed line. (e), (f), and (h) are the measured laser profiles in the $z = 0$, $y = 0$, and $x = 0$ planes, respectively. The white dashed line in (e) indicates the first dark ring of the Airy disk. (g) The laser intensity along the y axis ($x = z = 0$). Dots are the experimental data. The solid line is an Airy function for the diffraction by a circular aperture. The radius of the first dark ring is 740 nm.

phase constant. The parabolic phase can be shifted by integer numbers of 2π to reduce the phase range to 2π. The metalens is designed to have a diameter of 425 μm, a focal length of 100 μm, and an NA of 0.9 for a 1064 nm laser beam in vacuum. We create the metalens using amorphous silicon nanopillars [Fig. 1(b)], which have a large refractive index of 3.6 at 1064 nm. The silicon nanopillars work as antennas for the laser beam. The phase shift is controlled by the different diameters of the silicon antenna. The height of silicon nanopillars is 500 nm. Figure 1(d) reveals the simulated phase variation of the electric field propagation on both sides of the metalens. We deposit 500-nm-thick amorphous silicon on a sapphire substrate in a plasma-enhanced chemical vapor deposition (PECVD) tool under 220°C and create the nanopillars with e-beam lithography. These materials are compatible with an ultrahigh vacuum. Figure 1(b) shows a SEM image of a metalens that consists of multiple nanometer scale silicon antennas. Figure 1(c) shows an optical image of the metalens.

The laser profiles at the focal spot along different directions are measured to determine the NA of the metalens. To measure the NA of the metalens, a 1064 nm laser with a beam waist much larger than the diameter of the metalens is incident on the metalens. So, it is convenient to consider the incident beam as a plane wave with a constant amplitude. We use a conventional NA = 0.9 OBJ to collect the focused laser beam after the metalens and take images with a camera. The metalens is moved along z axis with a motorized actuator to measure the laser profile along the z axis. Figures 1(e), 1(f), and 1(h) present the measured laser profiles at the focal point in the $z = 0$, $y = 0$, and $x = 0$ planes, respectively. By fitting the first dark ring of the Airy's disc, the NA of the metalens is measured to be 0.88. Remarkably, the measured full width at half-maximum (FWHM = 1.8 μm) along the axial direction of a 1064 nm laser focused by our metalens is less than half of that (FWHM = 3.9 μm) for a 715 nm laser focused by a former metalens with a designed NA of 0.99 [17].

Now, we demonstrate the first observation of metalens-based optical levitation in vacuum. The experimental setup is shown in Fig. 2(a). The metalens is mounted on a translation stage. A 1064 nm laser beam is directed onto the metalens for optical levitation. A 532 nm laser illuminates the levitated nanoparticle for imaging with a conventional OBJ. The Gaussian beam diameter of the 1064 nm laser is adjusted to 425 μm to match the diameter of the metalens, which improves the levitation stability and trapping efficiency. The incident laser power at focus is around 200 mW.

In the experiment, silica nanoparticles with a diameter of 170 nm are used. The nanoparticles are diluted in deionized water and launched by an ultrasonic nebulizer for trapping. The metalens can successfully levitate nanoparticles even after repeated use. The inset of Fig. 2(a) shows an optical image of a trapped nanoparticle using the scattered light of the 532 nm laser. To measure the motion of a trapped nanoparticle, a set of balanced detectors collect the light backward scattered by the nanoparticle and the reflected light from the surface of the sapphire substrate of the metalens. The scattered light from the trapped particle interferes with the reflection light from the substrate, and, hence, we can measure the motion of the particles. Compared to the typical backward detection, which requires an additional independent reference laser beam for interference, the detection with the metalens system is much simpler and can be integrated to chip-based devices.

In the frequency domain, the power spectrum density (PSD) of the motion of a levitated nanoparticle is given by [22]

$$S_{qq}(\omega) = \frac{\Gamma_{\mathrm{CM}} k_{\mathrm{B}} T_{\mathrm{CM}}/\pi M}{(\omega^2 - \omega_{\mathrm{q}}^2)^2 + \Gamma_{\mathrm{CM}}^2 \omega^2},$$

where Γ_{CM} is the damping rate of the center-of-mass motion (COM), ω_{q} is the mechanical oscillation frequency of the trapped

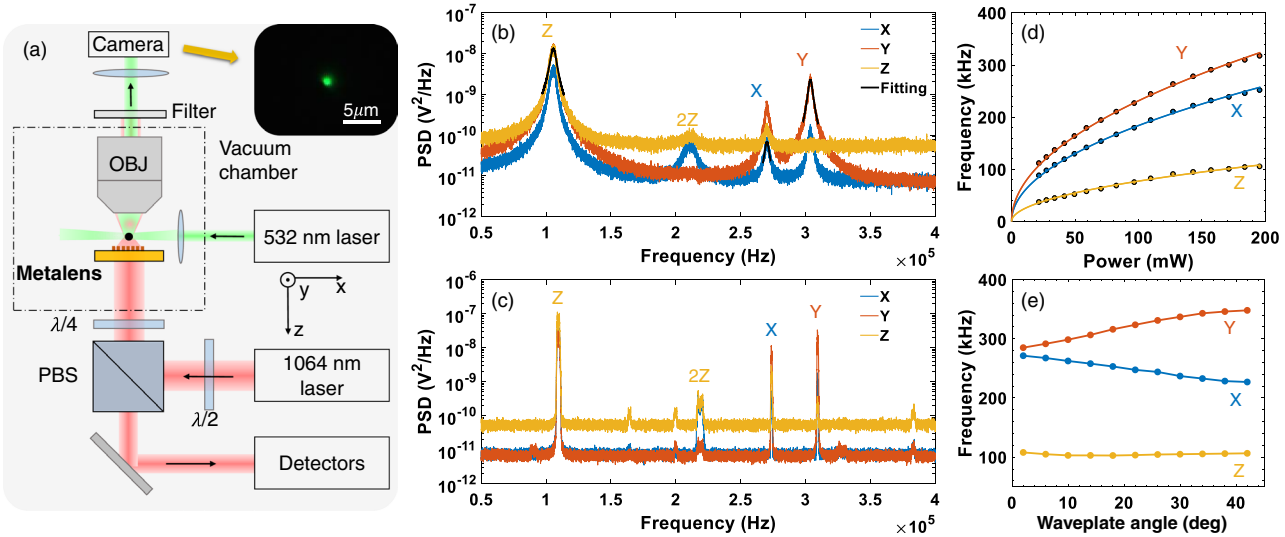

Fig. 2. (a) Schematics of the metalens-based optical levitation and detection system. A 1064 nm laser is used for optical levitation, and a 532 nm laser is used for imaging. The inset figure is the optical image of a levitated particle. PBS, polarizing beamsplitter; OBJ, objective lens. (b), (c) Power spectral density (PSD) of the mechanical motions of the levitated particle at 5 Torr and 5 mTorr with an elliptically polarized trapping laser. The black solid curves in (b) are the Lorentzian fittings. The peak around 215 kHz is the second-harmonic generation of the z peak. Other small peaks in (c) come from difference-frequency generations and sum-frequency generations. (d) The relationship between the trapping frequencies is shown as a function of the laser power. Solid lines are the fitting with a square root function. (e) The measured trapping frequencies are shown as a function of the laser polarization.

particle, T_{CM} is the temperature of COM, M is the mass of the particle, and k_B is the Boltzmann constant. Figures 2(b) and 2(c) are the PSD of the COM at the pressure of 5 Torr and 5 mTorr, respectively. The black solid curves are the Lorentzian fittings. The trapping frequencies for x, y, and z directions are 270 kHz, 304 kHz, and 106 kHz, respectively. They are higher than the frequencies achieved with a conventional NA = 0.9 OBJ at the same trapping laser power. Figure 2(d) shows that the trapping frequencies are proportional to the square root of laser power, which is similar to the case where the particle is trapped by the OBJ. Although our metalens is insensitive to the laser polarization, the vector electric field distribution and hence the trapping frequency in a tightly focused laser beam is related to the laser polarization. If the incident beam is linearly polarized, its trapping frequency in the y direction can reach up to 350 kHz, as shown in Fig. 2(e). The higher trapping frequency will be helpful for ground-state cooling. In addition, PSD in Figs. 2(b) and 2(c) shows that the trapping potential well is not perfectly harmonic. Strong nonlinear effects including second-harmonic generation are observed.

The transmitted beam from the center part of a lens contributes mainly to the scattering force. We may eliminate the central part of the beam without hurting optical levitation. In Figs. 3(a) and 3(b), we show a metalens with a hole at the center. The hole diameter is 60 μm. Experimentally, we find that the metalenses with a 60 μm hole has a better performance. It can trap a nanoparticle at a lower pressure than a metalens without a hole when there is no feedback cooling. Figure 3(c) is the PSD of a nanoparticle trapped at 2.0×10^{-4} Torr with a linearly polarized beam by metalens with a 60 μm hole.

We also realize optical levitation in a dual-beam trap and transfer a nanoparticle between two optical tweezers. One beam is focused by the metalens. The other trapping beam is implemented by a conventional OBJ, as shown in Fig. 4(a). The particle in the dual-beam trap can jump from one potential well to the other, depending on the laser power distribution. An optical image of the

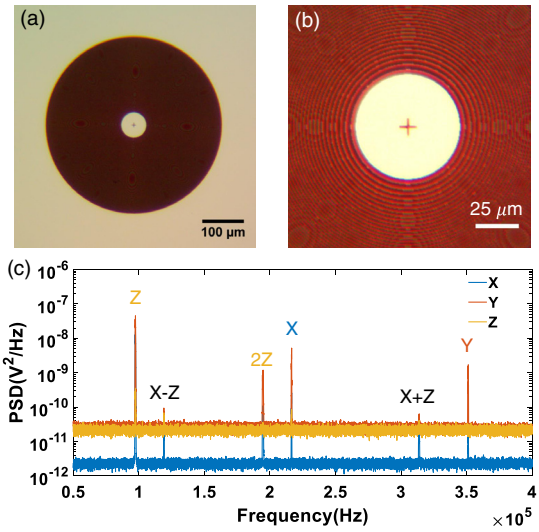

Fig. 3. (a), (b) Optical images of a metalens with a 60-μm-diameter hole at the center. The center cross mark is used for alignment. The focal length of the metalens is 100 μm. (c) PSD of a nanoparticle at 2.0×10^{-4} Torr with a linearly polarized incident beam. The trapping frequencies of x, y, and z motions are about 216, 351, and 97 kHz.

particle in a dual-beam trap is shown in Fig. 4(b). The separation between two potential wells is about 1.5 μm. In Fig. 4(c), we show the transfer process between two trapping wells by controlling laser power distribution. When the half-waveplate is at 0° (45°), all of the laser power is directed on the OBJ (metalens). Because the maximum trapping depth is large, the particle jumping happens when the laser power of one of the optical tweezers is close to zero.

In conclusion, we have demonstrated the first, to the best of our knowledge, experimental realization of metalens-based on-chip optical levitation of a nanoparticle in vacuum. Compared to a conventional OBJ, our metalens can work at more extreme conditions.

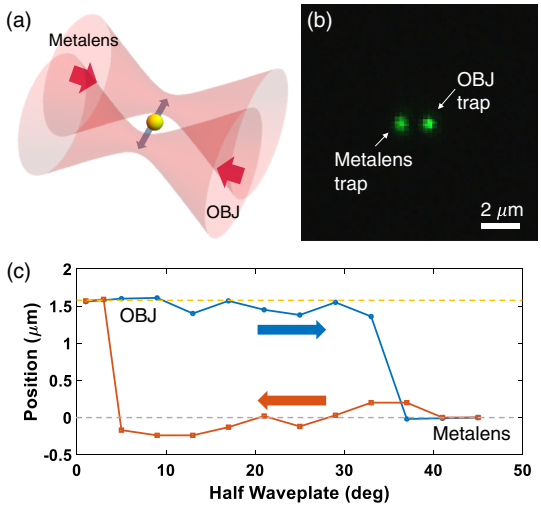

Fig. 4. (a) Scheme of a nanoparticle levitated by a dual-beam trap. (b) Optical image of a particle transferring between two potential wells. The left (right) green spot shows the particle was captured by the metalens (OBJ). The separation between two wells is about 1.5 μm. (c) The transfer process was adjusted by controlling the laser power distribution. Zero degrees (45°) of the half-waveplate means the total laser power was directed on the OBJ (metalens). The dashed yellow (gray) line is the steady trapping position for the OBJ (metalens) trap.

It also provides more freedom to generate complex trapping potentials with nanofabrication. Metalens levitation in vacuum can open more opportunities to study fundamental physics and applied science. For example, we can precisely control the distance between a surface and a trapped particle for studying surface interactions [11]. In addition, a high-NA metalens can potentially be used to create optical tweezers for trapping ultracold atoms in vacuum for quantum simulation [23].

Funding. Office of Naval Research (N00014-18-1-2371); National Science Foundation (PHY-2110591); Sandia National Laboratories (Laboratory Directed Research and Development program).

Acknowledgment. We thank Alejandro J. Grine and Francis Robicheaux for helpful discussions. This project is partially supported by the Laboratory Directed Research and Development program at Sandia National Laboratories, a multimission laboratory managed and operated by National Technology and Engineering Solutions of Sandia LLC, a wholly owned subsidiary of Honeywell International Inc., for the U.S. Department of Energy's National Nuclear Security Administration under Contract No. DE-NA0003525. This paper describes objective technical results and analysis. Any subjective views or opinions that might be expressed in the paper do not necessarily represent the views of the U.S. Department of Energy or the United States Government.

Disclosures. The authors declare no conflicts of interest.

Data Availability. Data underlying the results presented in this Letter are not publicly available at this time but may be obtained from the authors upon reasonable request.

REFERENCES

1. J. Millen, T. S. Monteiro, R. Pettit, and A. N. Vamivakas, Rep. Prog. Phys. **83**, 026401 (2020).
2. G. Ranjit, M. Cunningham, K. Casey, and A. A. Geraci, Phys. Rev. A **93**, 053801 (2016).
3. J. Ahn, Z. Xu, J. Bang, P. Ju, X. Gao, and T. Li, Nat. Nanotechnol. **15**, 89 (2020).
4. F. Monteiro, W. Li, G. Afek, C.-L. Li, M. Mossman, and D. C. Moore, Phys. Rev. A **101**, 053835 (2020).
5. Y. Zheng, L.-M. Zhou, Y. Dong, C.-W. Qiu, X.-D. Chen, G.-C. Guo, and F.-W. Sun, Phys. Rev. Lett. **124**, 223603 (2020).
6. J. Ahn, Z. Xu, J. Bang, Y.-H. Deng, T. M. Hoang, Q. Han, R.-M. Ma, and T. Li, Phys. Rev. Lett. **121**, 033603 (2018).
7. R. Reimann, M. Doderer, E. Hebestreit, R. Diehl, M. Frimmer, D. Windey, F. Tebbenjohanns, and L. Novotny, Phys. Rev. Lett. **121**, 033602 (2018).
8. F. Ricci, M. T. Cuairan, A. W. Schell, E. Hebestreit, R. A. Rica, N. Meyer, and R. Quidant, arXiv:2107.01084 (2021).
9. A. A. Rahman and P. Barker, Nat. Photonics **11**, 634 (2017).
10. U. Delić, M. Reisenbauer, K. Dare, D. Grass, V. Vuletić, N. Kiesel, and M. Aspelmeyer, Science **367**, 892 (2020).
11. Z. Xu, Z. Jacob, and T. Li, Nanophotonics **10**, 537 (2021).
12. S. Bose, A. Mazumdar, G. W. Morley, H. Ulbricht, M. Toroš, M. Paternostro, A. A. Geraci, P. F. Barker, M. S. Kim, and G. Milburn, Phys. Rev. Lett. **119**, 240401 (2017).
13. A. D. Rider, D. C. Moore, C. P. Blakemore, M. Louis, M. Lu, and G. Gratta, Phys. Rev. Lett. **117**, 101101 (2016).
14. N. Yu, P. Genevet, M. A. Kats, F. Aieta, J.-P. Tetienne, F. Capasso, and Z. Gaburro, Science **334**, 333 (2011).
15. X. Ni, Z. J. Wong, M. Mrejen, Y. Wang, and X. Zhang, Science **349**, 1310 (2015).
16. M. Khorasaninejad, W. T. Chen, R. C. Devlin, J. Oh, A. Y. Zhu, and F. Capasso, Science **352**, 1190 (2016).
17. R. Paniagua-Dominguez, Y. F. Yu, E. Khaidarov, S. Choi, V. Leong, R. M. Bakker, X. Liang, Y. H. Fu, V. Valuckas, L. A. Krivitsky, and A. I. Kuznetsov, Nano Lett. **18**, 2124 (2018).
18. H. Markovich, I. I. Shishkin, N. Hendler, and P. Ginzburg, Nano Lett. **18**, 5024 (2018).
19. G. Tkachenko, D. Stellinga, A. Ruskuc, M. Chen, K. Dholakia, and T. F. Krauss, Opt. Lett. **43**, 3224 (2018).
20. M. Plidschun, H. Ren, J. Kim, R. Förster, S. A. Maier, and M. A. Schmidt, Light Sci. Appl. **10**, 57 (2021).
21. C. Zhao, Opt. Express **25**, 2496 (2017).
22. T. Li, S. Kheifets, and M. G. Raizen, Nat. Phys. **7**, 527 (2011).
23. H. Bernien, S. Schwartz, A. Keesling, H. Levine, A. Omran, H. Pichler, S. Choi, A. S. Zibrov, M. Endres, M. Greiner, V. Vuletić, and M. D. Lukin, Nature **551**, 579 (2017).